Life Sciences 216 (2019) 75–84

Contents lists available at ScienceDirect

Life Sciences

journal homepage: www.elsevier.com/locate/lifescie

Overexpression of Forkhead box C1 attenuates oxidative stress, inflammation and apoptosis in chronic obstructive pulmonary disease

Shuyue Xia[a,*], Jian Qu[b], Hui Jia[a], Wei He[a], Jing Li[b], Long Zhao[a], Mingqing Mao[a], Yan Zhao[a]

[a] Department of Respiratory and Critical Care Medicine, Central Hospital Affiliated to Shenyang Medical College, Shenyang 110024, People's Republic of China
[b] Shenyang Environmental Monitor Central Station, Shenyang 110016, People's Republic of China

ARTICLE INFO

Keywords:
COPD
Foxc1
Oxidative stress
Inflammation
Apoptosis

ABSTRACT

Aim: Chronic obstructive pulmonary disease (COPD) is a disease caused by cigarette smoke, which has been emerging as a serious health problem worldwide. The aim of this study is to explore the mRNA expression profile of lung tissues from the COPD rats and to characterize the role of Forkhead box C1 (Foxc1) in COPD.

Main methods: Wistar rats were exposed to cigarette smoke during 16 weeks for COPD model establishment. The microarray was used to identify the differential gene expression in the lung of rats. Adenovirus carrying Foxc1 was administered to rats by intratracheally instillation once a week for 16 weeks. Human bronchial epithelial cell line (16HBE) cells were transfected with Foxc1 siRNA followed by incubation in the presence of CSE (10%) for 24 h. Subsequently, the pathological changes, fibrosis, apoptosis, inflammatory cytokines and oxidative stress were detected.

Key findings: Microarray results showed an upregulation of Foxc1 in lung tissues in COPD rats. Overexpression of Foxc1 mitigated the lung injury, as evidenced by reducing alveolar fusion, inflammatory cell infiltration and oxidative stress. Additionally, the apoptosis was remarkably increased in the lung in rats exposed to cigarette smoke, which was suppressed by Foxc1 overexpression. Furthermore, downregulation of Foxc1 aggravated the inflammation, oxidative stress and apoptosis in 16HBE cells with CSE treatment.

Significance: Overexpression of Foxc1 could prevent oxidative stress, inflammation responses and cell apoptosis and knockdown of Foxc1 has the opposite effect, suggesting that Foxc1 may be available for lung protection during COPD.

1. Introduction

Chronic obstructive pulmonary disease (COPD) is characterized by chronic airflow obstruction, exercise intolerance, and shortness of breath on exertion, and is one of the most incident and fateful diseases in the world [1]. The Global Burden of Disease Study demonstrated that the incidence of COPD is > 250 million, with a mortality of about 3 million in 2016 [2,3]. It is noteworthy that COPD is now the fourth-ranked cause of death worldwide [4] and ranked among the top three leading causes of death in China [5]. COPD is a multidimensional disease, with tissue damage involving complex interactions among inflammation, oxidative stress, and apoptosis, and so on [6]. The pathogenesis is not fully elucidated, while the typical risk factor for COPD is cigarette smoking [7]. Recent studies demonstrated that cigarette smoke induced inflammation in lung tissues in mice and increased the rate of decline in lung function [8,9].

Forkhead box C1 (Foxc1) is one member of the Forkhead box (Fox) gene family of transcription factors [10], which has a transcriptional inhibitory domain in the central region and two transcriptional activation domains at the ends of the molecule [11]. Foxc1 is closely related to the occurrence of various pathophysiological processes, such as cancer [12,13], endochondral ossification [14], and tooth specification [15]. Recent studies further demonstrated that Foxc1 was involved in resisting oxidative stress and apoptosis in eye disease [16,17].

In this study, we identified the differential gene expression between the lung tissues in rats exposed to cigarette smoke and the controls, and then found that Foxc1 was highly expressed in the COPD rats. In addition, cigarette smoke induced lung tissue injury, including obvious inflammatory cell infiltration, alveolar expansion, elevations in inflammatory cytokines, oxidative stress and apoptosis, which can be attenuated by Foxc1 overexpression. Moreover, the beneficial role of Foxc1 was further validated by downregulation of Foxc1 in 16HBE cells

* Corresponding author at: Department of Respiratory and Critical Care Medicine, Central Hospital Affiliated to Shenyang Medical College, 5 West Nanqi Road, Shenyang 110024, People's Republic of China.
E-mail address: Syx262@126.com (S. Xia).

https://doi.org/10.1016/j.lfs.2018.11.023
Received 26 July 2018; Received in revised form 2 November 2018; Accepted 10 November 2018
Available online 11 November 2018
0024-3205/

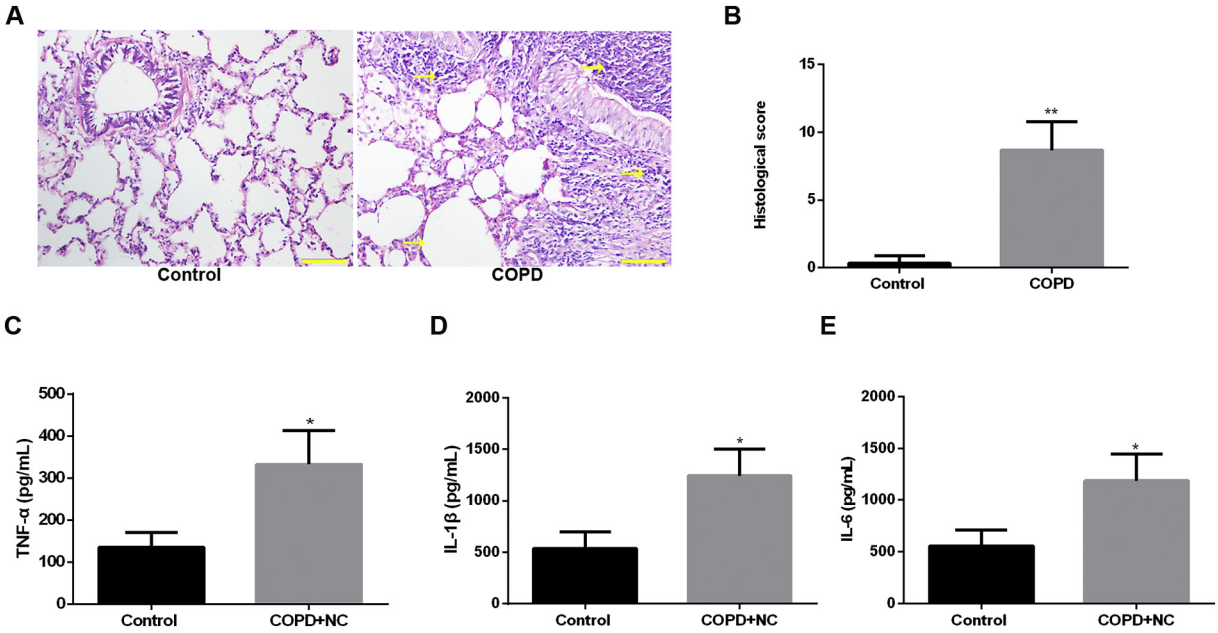

Fig. 1. Establishment of COPD by cigarette smoke exposure in rats
Wistar rats were exposed to cigarette smoke or room air for 16 weeks, the blood samples and the lung tissues were obtained from rats in control and COPD groups. (A) H&E staining showed marked inflammatory infiltrate, enlarged alveolar spaces, and thicken alveolar walls in the lung of rats exposed to cigarette smoke (×200 magnification, scale bar: 100 μm). (B) The histological changes between the COPD group and the controls were scored. (C–E) The levels of TNF-α, IL-1β and IL-6 in serum were determined by ELISA. The values are expressed as means ± STDEV (N = 3/group). $^{*}P < 0.05$ vs Control, $^{**}P < 0.01$ vs Control.

with CSE treatment. Therefore, Foxc1 was effective in protection of lung tissue injury in COPD rats in terms of antioxidant, anti-inflammatory, and anti-apoptotic responses.

2. Materials and methods

2.1. Animals

8-week-old Wistar rats were obtained from the BEIJING HFK BIOSCIENCE CO., LTD, SCXK(JING)2014-0004 and all procedures were approved by the Ethics Review Committee for Central Hospital Affiliated to Shenyang Medical College. Rats were randomly divided into four groups (N = 3/Group for microarray and N = 6/Group for other experiments in vivo): the control group, the COPD group, the COPD + NC group, and the COPD + Foxc1 group. COPD model was established by exposing the rats to cigarette smoke. Briefly, the rats were placed in the sealed whole-body experimental smoking chamber (80 × 60 × 58 cm) and exposed to the smoke of twenty cigarettes (Huangguoshu cigarettes, 15 mg tar, and 1.2 mg nicotine each cigarette, Shenyang, China) for 50 min, twice daily for 16 weeks. Control rats were exposed to room air following the same schedule as previous description. For COPD + Foxc1 and COPD + NC groups, an adenovirus containing Foxc1 or negative control viruses (10^8 pfu/500 μl, Wanleibio, Shenyang, China) was instilled via trachea through the mouth of rats under anesthesia with 50 mg/kg of pentobarbital once a week and rats were treated with cigarette smoke for 16 weeks simultaneously. After 16 weeks of cigarette smoke exposure, blood samples were collected under anesthesia, all rats were then sacrificed intraperitoneally with 250 mg/kg of pentobarbital and the lung tissues were collected for the subsequent experiments. In the microarray analysis, normal Wistar rats were as control. In the second sets of experiments, Wistar rats received negative control viruses without cigarette smoke exposed were as the controls.

2.2. Hematoxylin-eosin (HE) and Masson staining

For HE staining, lung tissues were fixed in 10% formaldehyde, embedded in paraffin, sectioned into consecutive 5-μm-thick, and then stained with hematoxylin and eosin for histological analysis. For Masson staining, the sections were stained with acidic ponceau reagent (Sinopharm, Beijing, China) to evaluate the fibrosis in each group. The sections at 200× magnification were photographed with a microscope (Olympus, Tokyo, Japan). The histological changes detected by H&E staining in lung tissues between the COPD group and the controls were scored as described previously [18] and the degree of fibrosis was quantified by Image-Pro plus.

2.3. Preparation of cigarette smoking extracts (CSE)

CSE was prepared as described previously [19]. Briefly, Smoke from two cigarettes (Huangguoshu cigarettes) was bubbled through 25 ml serum free Keratinocyte medium (ScienCell, San Diego, CA, USA) as 100% CSE. The CSE was freshly prepared and sterilized using a 0.22 μm filter (Millipore, Boston, MA, USA) before treatment.

2.4. Cell culture

Human bronchial epithelial cell line 16HBE (Zhongqiaoxinzhou, Shanghai, China) was cultured in Keratinocyte medium in an atmosphere of 95% air and 5% CO_2 at 37 °C. After adhered to the plates, the 16HBE cells were transfected with Foxc1 siRNA or negative control sequence, followed by incubation in the presence or absence of CSE (10%) for 24 h.

2.5. Oxidative stress index and cytokine measurement

Activities of superoxide dismutase (SOD) and concentrations of malondialdehyde (MDA) in lung tissues and cell lysates were determined via commercial kits (Nanjing Jiancheng Bioengineering Institute, Nanjing, China). Concentrations of tumor necrosis factor (TNF-α), interleukin (IL)-1β and IL-6 in serum and cell culture supernatant were measured according to the instruction of the commercial Enzyme-linked immunosorbent assay (ELISA) kits (MULTI SCIENCES, Hangzhou, China).

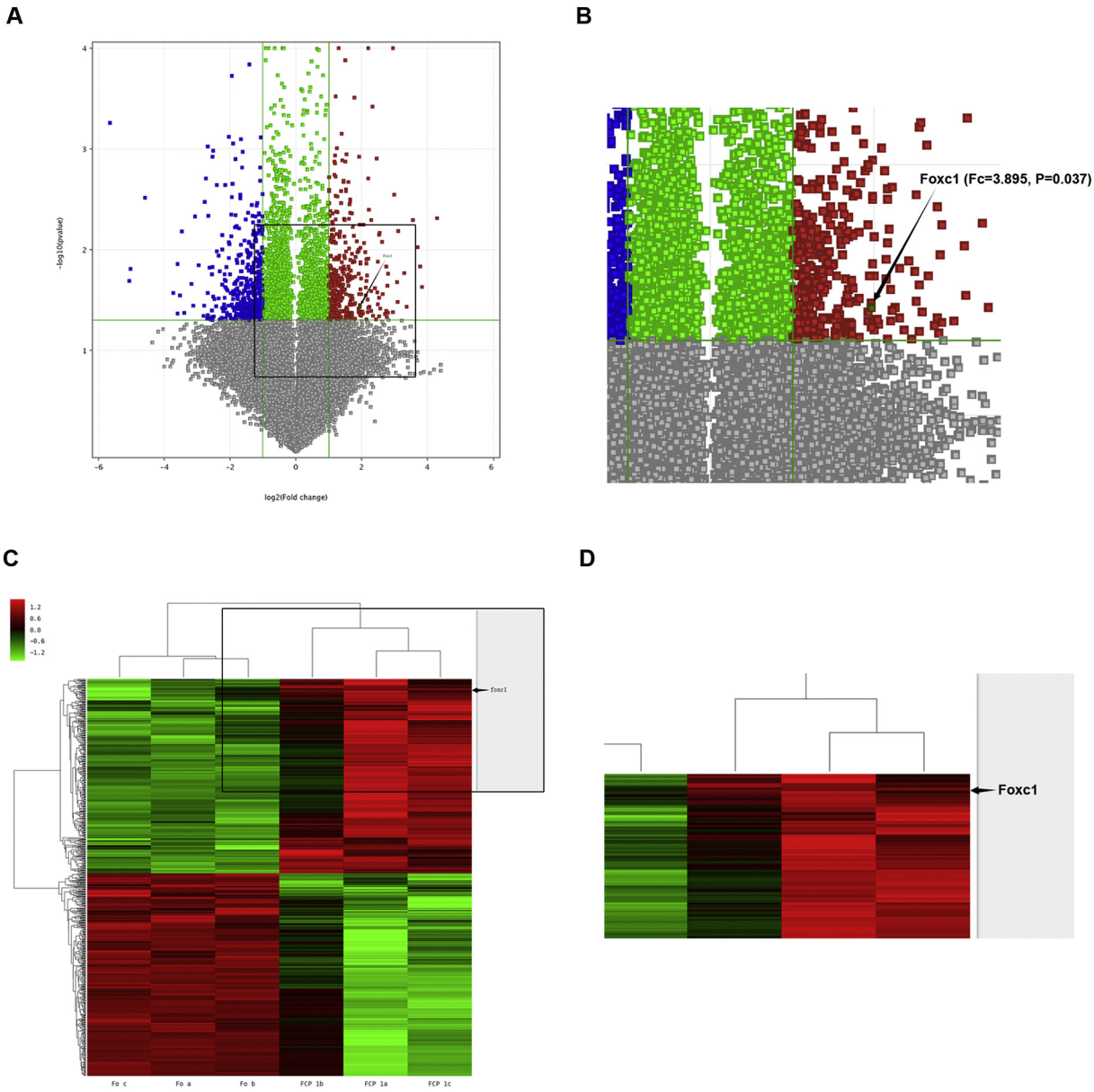

Fig. 2. Microarray analysis of the lung in rats exposed to cigarette smoke
The lung tissues of rats in COPD or the controls were performed with microarray analysis. (A) The analyzed genes were presented in a volcano plot. The negative log10 *P* value was plotted on the y-axis, and log2 fold change was plotted on the x-axis. The red and blue depicts genes with a fold change ≥ 2, *P* value ≤ 0.05. (B) The magnified picture of the volcano plot. (C) The cluster analysis of microarray data was shown in the heat map. Each row represents a gene and each column represents a single tissue. Red colour indicated the mRNA levels were higher than the median, while black indicated equal and green indicated a lower level. (D) The magnified picture of the heat map. (N = 3/group). (For interpretation of the references to colour in this figure legend, the reader is referred to the web version of this article.)

2.6. Microarray procedure and analysis

Total RNAs were isolated from lung tissues by using mirVanaTM RNA Isolation Kit (Thermo Scientific, Pittsburgh, PA, USA), purified with an RNeasy Mini Kit (Qiagen, Hilden, Germany) and quantified by the NanoDrop ND-2000 (Thermo Scientific). The RNA integrity was assessed by using Agilent Bioanalyzer 2100 (Agilent Technologies, Santa Clara, CA, USA) with 28S/18S ratio ≥ 1.5 and RNA Integrity Number (RIN) ≥ 8.1. The Agilent SurePrint G3 Rat GE V2.0 Microarray was used in this experiment according to the manufacturer's protocols. Feature Extraction software (version10.7.1.1, Agilent Technologies) was used to analyze array images to get raw data and Genespring (version13.1, Agilent Technologies) was employed for basic analysis with the raw data. *t*-test was used to identify genes with a fold change ≥ 2.0 and a *P* value ≤ 0.05.

2.7. Quantitative real-time RT-PCR

For quantitative analysis of gene expression, RNAs were extracted with Trizol from lung tissues and cell lysates. The cDNA was synthesized from the total RNA using a Super M-MLV reverse transcriptase (BioTeke, Beijing, China) in presence of random primers and oligo $(dT)_{15}$. Primer sequences were as follows: Rat Foxc1 Forward: TGGAC CGCTTTCCCTTCTATC, Rat Foxc1 Reverse: GCCCTTGCCTGGCTTCTT, Human Foxc1 Forward: ACAGCATCCGCCACAACCTC, Human Foxc1 Reverse: TGTCCTTCACCGCGTCCTTC, Rat β-actin Forward: GGAGATT ACTGCCCTGGCTCCTAGC, Rat β-actin Reverse: GGCCGGACTCATCGT ACTCCTGCTT, Human β-actin Forward: CTTAGTTGCGTTACACCCTTT

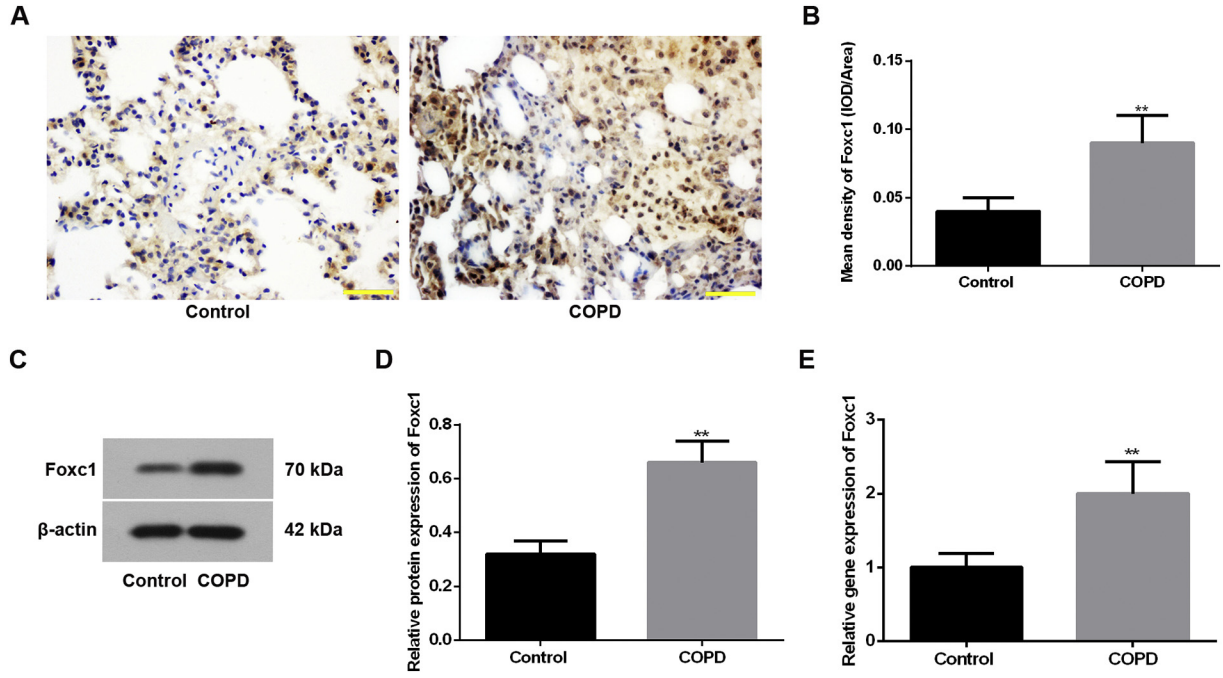

Fig. 3. Cigarette smoke exposure enhances Foxc1 expression in the lung in rats.
The expression of Foxc1 in lung tissues in Wistar rats with or without cigarette smoke exposure for 16 weeks were examined. (A) Immunohistochemical staining was performed to detect the protein expression of Foxc1 in the lung from each group and examined microscopically under a 400× lens (scale bar: 50 μm). The brown-yellow nuclear stain was the expression of Foxc1. (B) The Foxc1 expression levels were quantified by Image-Pro Plus. (C)Western blot analysis was used to determine the protein expression level of Foxc1. (D) The band intensity ratio of the western blot was calculated with β-actin as the internal control. (E) The mRNA expression of Foxc1 in the lung in each group was determined by real-time PCR, with β-actin as the internal control. The values are expressed as means ± STDEV ($N = 6$/group). $^{**}P < 0.01$ vs Control. (For interpretation of the references to colour in this figure legend, the reader is referred to the web version of this article.)

CTTG, Human β-actin Reverse: CTGTCACCTTCACCGTTCCAGTTT. Subsequently, the real-time PCR reaction system was established with SYBR Green (Solarbio, Beijing, China) and 2 × Power Taq PCR MasterMix (BioTeke), which then analyzed on Exicycler 96 Real-Time Quantitative PCR Thermal Block (Bioneer, Daejeon, Korea). All data were analyzed using the $2^{-\triangle\triangle Ct}$ method and the expression of β-actin was used as the internal control.

2.8. Immunohistochemistry and TUNEL assay

The lung tissues were cut into sections of 5 μm as previously described. Following antigen retrieval, lung sections were treated with 3% hydrogen peroxide for 15 min and blocked with goat serum. Subsequently, the sections were incubated with the Foxc1 antibody (1: 500, Abcam, Cambridge, England) at 4 °C overnight, followed by incubation with the biotin-labeled secondary antibody (Beyotime, Shanghai, China) and horseradish peroxidase (HRP)-conjugated streptavidin (Beyotime) at 37 °C for 30 min. Finally, the signals were visualized with DAB (Solarbio) and counter-stained with hematoxylin, and then observed under a light microscopy at 400× magnification. The quantitative image analysis was performed by Image-Pro Plus.

A commercial In Situ Cell Death Detection Kit (Roche, Basel, Switzerland) was used to detect the apoptotic cells in the lung and 16HBE cells. In vivo experiment, the rat lung slices were dewaxed in xylene and then permeabilized by incubating with 0.1% Triton X–100 (Beyotime). The broken DNA strands were labeled by incubating the slices with TUNEL reaction mix according to the manufacturer's instruction of the kit (Roche, Basel, Switzerland). After staining with 4′, 6-diamidino-2-phenylindole (DAPI, biosharp, Hefei, China), the sections were photographed at 400× magnification under an immunofluorescence microscopy (Olympus). In vitro experiment, the 16HBE cells were cultured on glass slides for confluence and fixed with 4% paraformaldehyde (Sinopharm) for 15 min. After permeating with 0.1% Triton X–100 (Beyotime), the apoptotic cells were detected with In Situ Cell Death Detection Kit (Roche) followed by staining with hematoxylin (Solarbio), and then observed under a microscope at 200× magnification.

2.9. Protein extraction and immunoblot

Total proteins from lung tissues and cell lysates were extracted by RIPA lysis buffer (Beyotime) and quantitated using BCA assay (Beyotime). For western blot, 40 μg of protein was loaded on sodium dodecyl sulfate-polyacrylamide gel electrophoresis (SDS-PAGE), and then transferred onto polyvinylidene fluoride (PVDF) membranes (Millipore, Billerica, MA, USA). The membranes were incubated with primary antibodies including Foxc1 (1:1000, Abcam), Bax (1:1000, Cell Signaling TECHNOLOGY, Massachusetts, USA), Bcl-2, Cleaved caspase-3 (1:500, Abcam) and β-actin (1:500, Bioss, Beijing, China) at 4 °C overnight. Subsequently, the members were treated with goat anti-rabbit or goat anti-mouse linked to HRP-conjugated secondary antibodies (1:5000, Beyotime). Finally, protein bands were visualized with chemiluminescence (ECL) reagent (Beyotime) and band density was quantified with Gel-Pro-Analyzer software. β-actin was served as the cellular internal control.

2.10. Statistical analysis

Data were expressed as the mean ± SD and analyzed with GraphPad Prism 6.0 software. Differences between the groups were performed using a *t*-test or one-way analysis of variance (ANOVA). Significance was accepted when P values < 0.05.

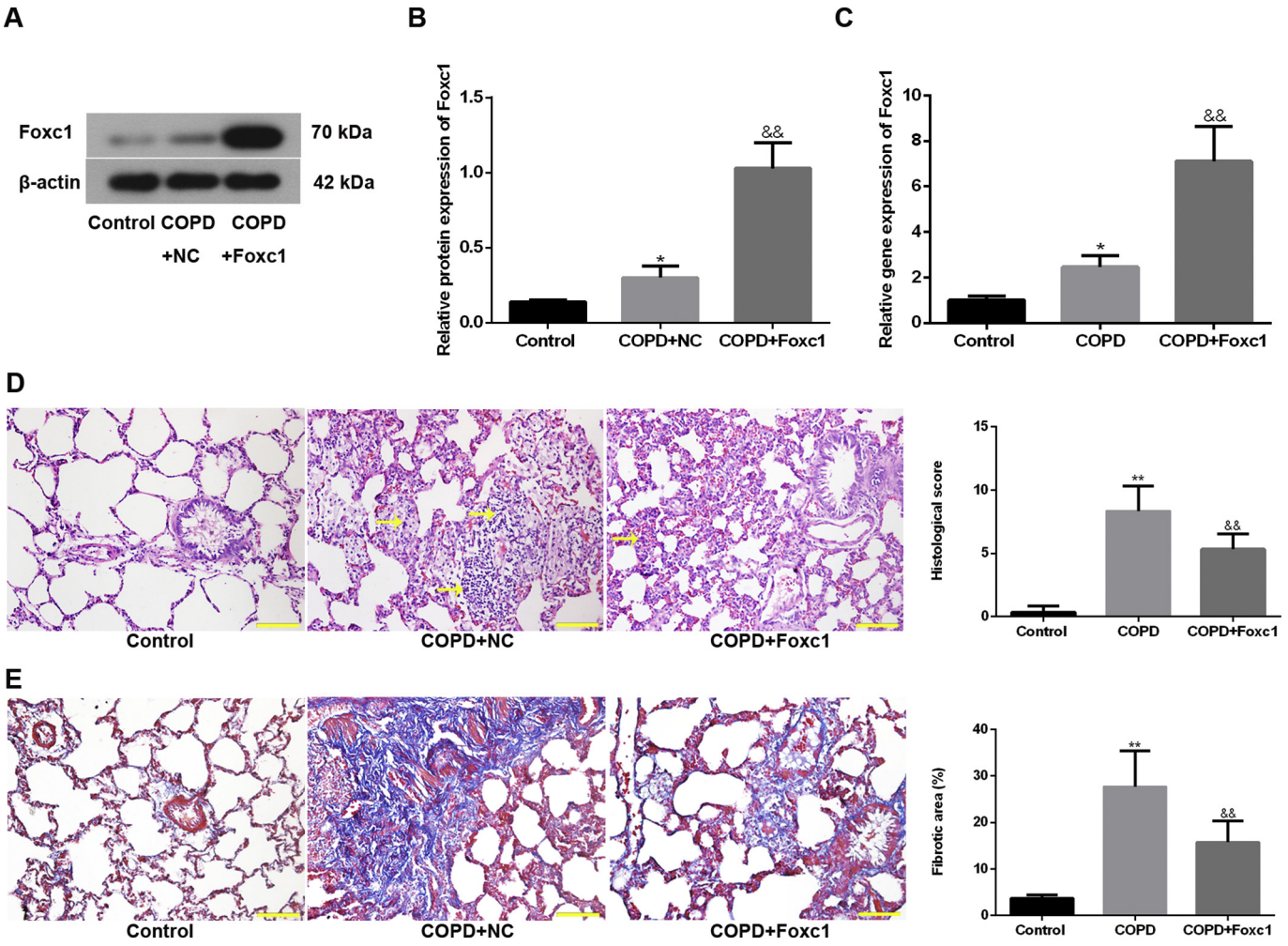

Fig. 4. Overexpression of Foxc1 alleviates pathological damage and fibrosis induced by cigarette smoke in lung
Wistar rats received adenovirus carring Foxc1 or negative control by intratracheal instillation through the mouth once a week, concurrently exposed to cigarette smoke. Wistar rats with negative control viruses treatment and exposed to room air as the controls (N = 6/group). After 16 weeks, blood samples were collected under anesthesia, all rats were then sacrificed and the lung tissues were collected. The levels of (A) Foxc1 protein in the lung from each group were monitored by western blot and (B) statistical analyses of brand intensity were presented, with β-actin as the internal control. (C) The mRNA levels of Foxc1 were measured by real-time PCR and β-actin served as the cellular internal control. (D) Histological changes in the lung in rats were shown with H&E staining and (E) the degree of fibrosis of the lung was assessed by Masson staining. The images were photographed at 200 × magnification (scale bar: 100 μm). The values are expressed as means ± STDEV. $^{*}P < 0.05$ vs Control, $^{**}P < 0.01$ vs Control; $^{\&\&}P < 0.01$ vs COPD + NC.

3. Results

3.1. Successful establishment of COPD in rats

With the purpose to confirm the impacts of cigarette smoke exposure on lung tissues in rats, sections of lung tissues were prepared for histological analysis and serum samples were detected for inflammatory reactions in both control and COPD groups. Exposure to cigarette smoke resulted in thicken alveolar walls, enlarged alveolar spaces and marked inflammatory infiltrate (Fig. 1A–B). Furthermore, the levels of TNF-α, IL-1β, and IL-6 in the serum from cigarette smoke-treated rats were markedly higher than those of controls, which were increased by 1.466 ± 0.319 folds, 1.370 ± 0.330 folds, and 1.181 ± 0.435 folds, respectively. These results indicated the successful establishment of COPD in rats (Fig. 1C-1E).

3.2. Identification of differentially expressed gene by microarrays

Abnormal gene expression occurs frequently in COPD. As shown in Fig. 2A–B, volcano plot demonstrated all the differentially expressed genes. Compared with the control group, 880 genes had an abnormal expression in the COPD lung tissues (Fold change ≥ 2, *P* value ≤ 0.05), specifically, 405 genes were found to be upregulated, while 475 genes were downregulated. Then, unsupervised hierarchical clustering analysis were performed on the differently expressed genes, and the data were shown as a heat map (Fig. 2C–D), indicating that samples obtained from the same condition had similar gene expression patterns. The results of the differential gene expression between the lung tissues in rats exposed to cigarette smoke and the controls were supplied as a Supplementary Table 1. One of the differently expressed genes was Foxc1, which was increased by 3.895 fold. To identify the anti-oxidative and anti-apoptotic effects of Foxc1, we performed overexpression and downregulation of Foxc1 for the subsequent experiments.

3.3. Cigarette smoke enhanced Foxc1 expression in rat lung tissues

In order to verify the effect of cigarette smoke on Foxc1 expression in lung tissues of rats, the expressions of Foxc1 in the control group and the COPD group were determined by immunohistochemistry, western blot, and real-time PCR. After 16 weeks of cigarette smoke exposure, markedly increased immunoactivity of Foxc1 was detected in lung tissues of COPD rats compared with the controls (Fig. 3A–B). Similarly,

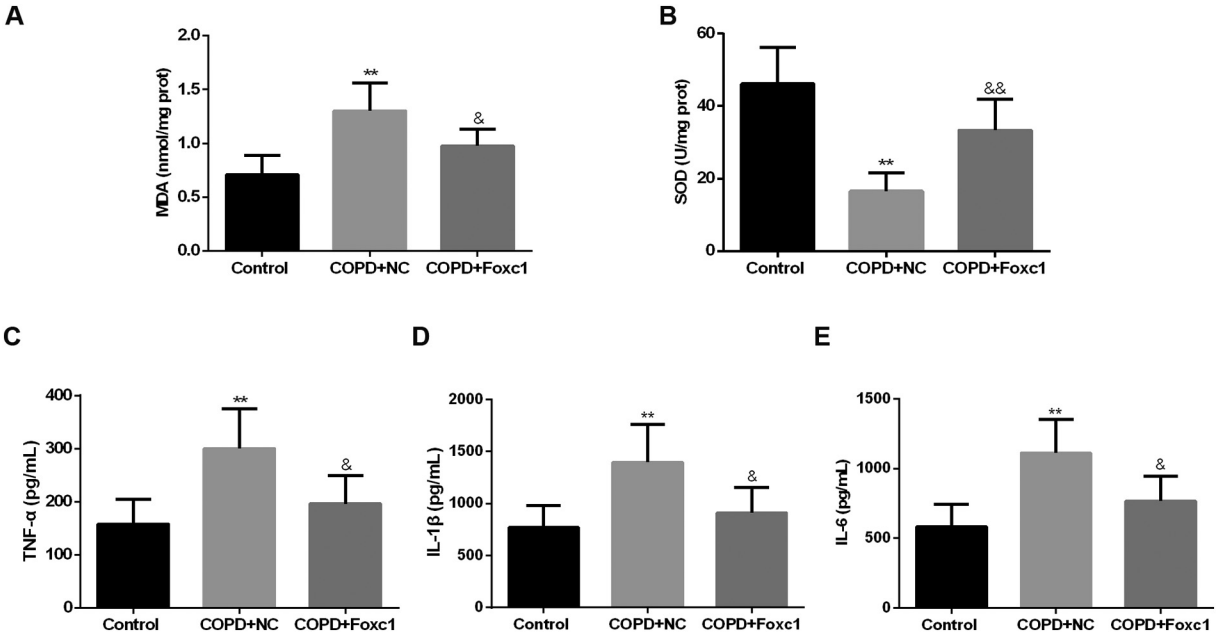

Fig. 5. Foxc1 overexpression attenuates cigarette smoke-induced lung oxidation and inflammation.
Wistar rats with adenovirus carring Foxc1 or negative control were exposed to cigarette smoke or room air for 16 weeks. Subsequently, the blood samples and the lung tissues were obtained. The (A) concentration of MDA and (B) activity of SOD in the lung tissues of rats were detected by commercial kits. The levels of cytokines of (C) TNF-α, (D) IL-1β, and (E) IL-6 in serum were analyzed by ELISA. The values are expressed as means ± STDEV ($N = 6$/group) $^{**}P < 0.01$ vs Control; $^{\&}P < 0.05$ vs COPD + NC, $^{\&\&}P < 0.01$ vs COPD + NC.

elevated Foxc1 protein and mRNA levels were also examined in the lungs of COPD rats (Fig. 3C–E). These data suggested that Foxc1 was upregulated in cigarette smoke-treated lung tissues in rats.

3.4. Overexpression of Foxc1 attenuated histological alterations in rats exposed to cigarette smoke

A Foxc1 expression construct was delivered into the lung via adenovirus to generate Foxc1 overexpression in lung. As shown in Fig. 4A–C, Foxc1 adenovirus induced a tremendous upregulation in protein and gene expressions. Subsequently, the morphological changes in lung tissues were observed with H&E staining. Fig. 4D showed a normal structure in the control rats, while the lung tissue was notably damaged in rats with cigarette smoke exposure, in which there was severe infiltration of inflammatory cells, accompanied by significant fusion and expansion of alveolar. Foxc1 overexpression over the course of COPD led to further decreases in excessive inflammatory infiltration. Moreover, Masson staining was used to determine the lung fibrosis. Obvious fibrosis presented in the cigarette smoke-treated lung was alleviated by overexpression of Foxc1 (Fig. 4E). These results demonstrated that Foxc1 overexpression mitigated the cigarette smoke-induced pulmonary damage in the COPD rat model.

3.5. Foxc1 overexpression alleviated inflammatory reaction and oxidative stress in COPD

The impacts of Foxc1 on COPD in rats were assessed by monitoring oxidative stress damage and inflammation in the lung. Sixteen-week cigarette smoke exposure significantly increased MDA (a predominant by-product of lipid peroxidation) concentration and decreased SOD (an essential antioxidant) activity in lung tissues of rats (Fig. 5A–B). In addition, increases in TNF-α, IL-1β, and IL-6 were found in the serum in COPD rats (Fig. 5C–E). In contrast, overexpression of Foxc1 partially counteracted cigarette smoke-induced damages of oxidative stress and inflammation in rats exposed with cigarette smoke. Furthermore, knockdown of Foxc1 increased the levels of inflammation and oxidative stress in 16HBE cells (Fig. 6). Taken together, these data showed a potent protective effect of Foxc1 in lung and 16HBE cells under cigarette smoke exposure.

3.6. Overexpression of Foxc1 suppressed the apoptosis in COPD

Apoptosis has been observed in COPD experimental animal models. Thus we further performed the TUNEL assay for evaluating the apoptosis in the lung in rats exposed to cigarette smoke. Following 16 weeks of cigarette smoke exposure, the number of TUNEL-positive cells in the lung tissue was obviously higher in the COPD rats than that in the controls (Fig. 7A and B). Furthermore, the apoptosis-related indicators such as Bax, Bcl-2, and Cleaved-caspase-3 were detected by western blot. Consistent with the TUNEL results, the expressions of Bax and Cleaved-caspase-3, as pro-apoptotic proteins, were upregulated in the lung in rats exposed to cigarette smoke, while the expression of Bcl-2, as an anti-apoptotic protein, was downregulated. Moreover, overexpression of Foxc1 decreased the caspase-3 cleavage and Bax expressions as well as increased Bcl-2 expression (Fig. 7C–7E). Meanwhile, downregulation of Foxc1 significantly aggravated CSE induced apoptosis in 16HBE cells (Fig. 8). The above results implied that Foxc1 overexpression inhibited the apoptosis in the lung of rats and 16HBE cells with COPD injury.

4. Discussion

Cigarette smoke may cause the chronic pulmonary disease, such as COPD [20]. The objective of this research is to explore the effects of cigarette smoke exposure on the lung and evaluate the potential therapy for COPD. Initially, in this study, we identified the differentially expressed genes in COPD and found that 16-week repeated cigarette smoke exposure enhanced Foxc1 expression in rat lung Moreover, overexpression of Foxc1 abrogated cigarette smoke-induced oxidative stress, inflammation, and subsequently alleviated apoptosis in the lung in rats. Furthermore, downregulation of Foxc1 aggravated the inflammation, oxidative stress and apoptosis in 16HBE cells with CSE treatment.

Microarray analysis is an available approach to offer multiplex

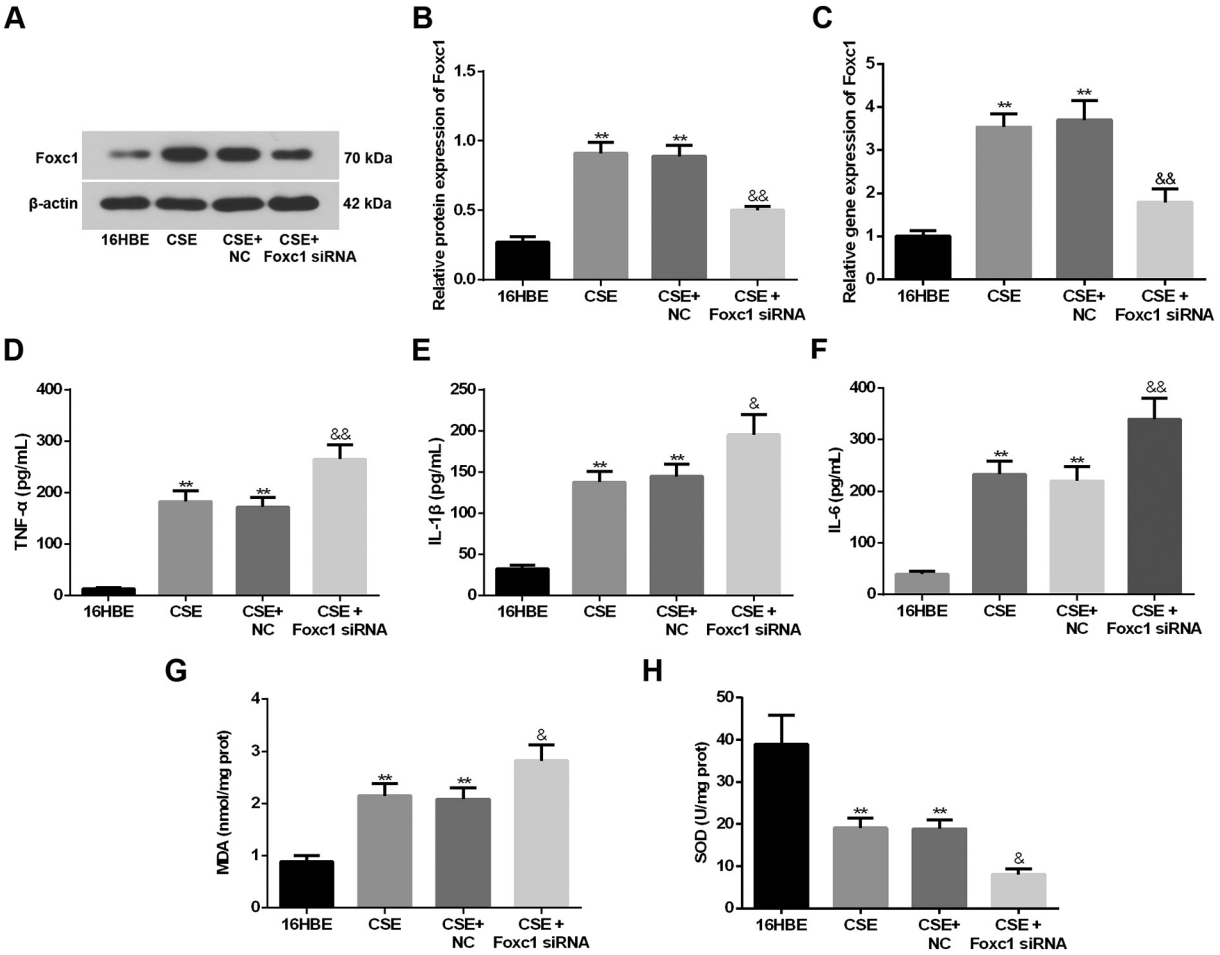

Fig. 6. Foxc1 downregulation accentated CSE-induced oxidation and inflammation in 16HBE cells.
16HBE cells were transfected with Foxc1 siRNA or negative control sequence. Subsequently, 16HBE cells were incubated in the presence and absence of CSE (10%) for 24 h. (A) Foxc1 protein expression in the 16HBE cells were examined by western blot and (B) statistical analyses of brand intensity were presented. (C) The mRNA levels of Foxc1 were detected by real-time PCR. β-actin served as the cellular internal control for western blot and real-time PCR. The levels of cytokines of (D) TNF-α, (E) IL-1β, and (F) IL-6 in cell supernatant were analyzed by ELISA. The (G) concentration of MDA and (H) activity of SOD in the 16HBE cells were assayed by commercial kits. The values are expressed as means ± STDEV ($N = 3$/group) $^{**}P < 0.01$ vs 16HBE; $^{\&}P < 0.05$ vs CSE + NC, $^{\&\&}P < 0.01$ vs CSE + NC.

detection that clarifies molecular changes in disease states [21,22]. In this study, microarray analysis of lung tissue in rats between the COPD group and the control group identified a number of differentially expressed genes. Especially, Foxc1 was one of the genes which were upregulated in the COPD group. Foxc1 was discovered to have a high expression in basal-like breast cancer (BLBC) and serve as a theranostic biomarker for BLBC [23]. Xia and co-workers showed that Foxc1 was highly expressed in hepatocarcinoma tissues and overexpression of Foxc1 promoted tumor metastasis indicating a poor prognosis [24]. In addition, Wang and co-authors demonstrated that Foxc1 promoted cell proliferation and invasion in human cervical cancer [25]. As far as we know, there is no report about the effect of Foxc1 in COPD. Herein, by performing microarray, immunohistochemistry, western blot, and real-time PCR, we confirm that Foxc1 is significantly unregulated in lung tissues in COPD rats and overexpression of Foxc1 alleviate the lung injury induced by cigarette smoke, suggesting the self-protection of the upregulation of Foxc1 in COPD.

All patients with COPD had the characteristics of elevated oxidative stress and inflammation [26]. Recent studies showed that increased oxidative damage in smokers contributed to lung injury through a variety of biological actions, and indexes of oxidative stress, such as ROS, MDA and SOD, were elevated in patients with COPD [27–29]. Interestingly, it has been reported that Foxc1 is required for cells in response to oxidative stress and downregulation of Foxc1 resulted in a reduction in cell viability in the eye through the transcriptional regulation of FOXO1A [16]. In line with previous studies, the concentration of MDA was elevated in lung tissues of the COPD rats and the activity of SOD was decreased compared with the control group. Moreover, Foxc1 overexpression inhibited the oxidative damage induced by cigarette smoke in COPD. Furthermore, lung damage resulted from cigarette smoke-associated airway inflammation had got relatively complete and deep research. Cigarette smoke directly promoted plasmacytoid dendritic cells maturation and the release of IL-6 in vitro [30], as well as induced an increase in cytokines including TNF-α, IL-1β, and IL-6 in serum and lung in mice [28,31]. As shown in the present study, overexpression of Foxc1 significantly decreased the excessive inflammation induced by cigarette smoke. To the best of our knowledge, our data for the first time demonstrate the anti-oxidant and anti-inflammatory properties of Foxc1 in COPD, which shed a new light on the role of Foxc1 in cigarette smoke-induced COPD.

An increasing number of studies indicated that pulmonary epithelial cell and vascular endothelial cell apoptosis resulted in airspace enlargement and alveolar wall damage [32,33]. In disease states, augmented apoptosis resulted in the loss of cells and the destruction of overall organization leading to cigarette smoke-induced lung injury [34], The apoptosis was showed to be induced by downregulation of Foxc1 in several cancer models such as lung cancer [35], salivary adenoid cystic carcinoma [36], and human cervical cancer [25].

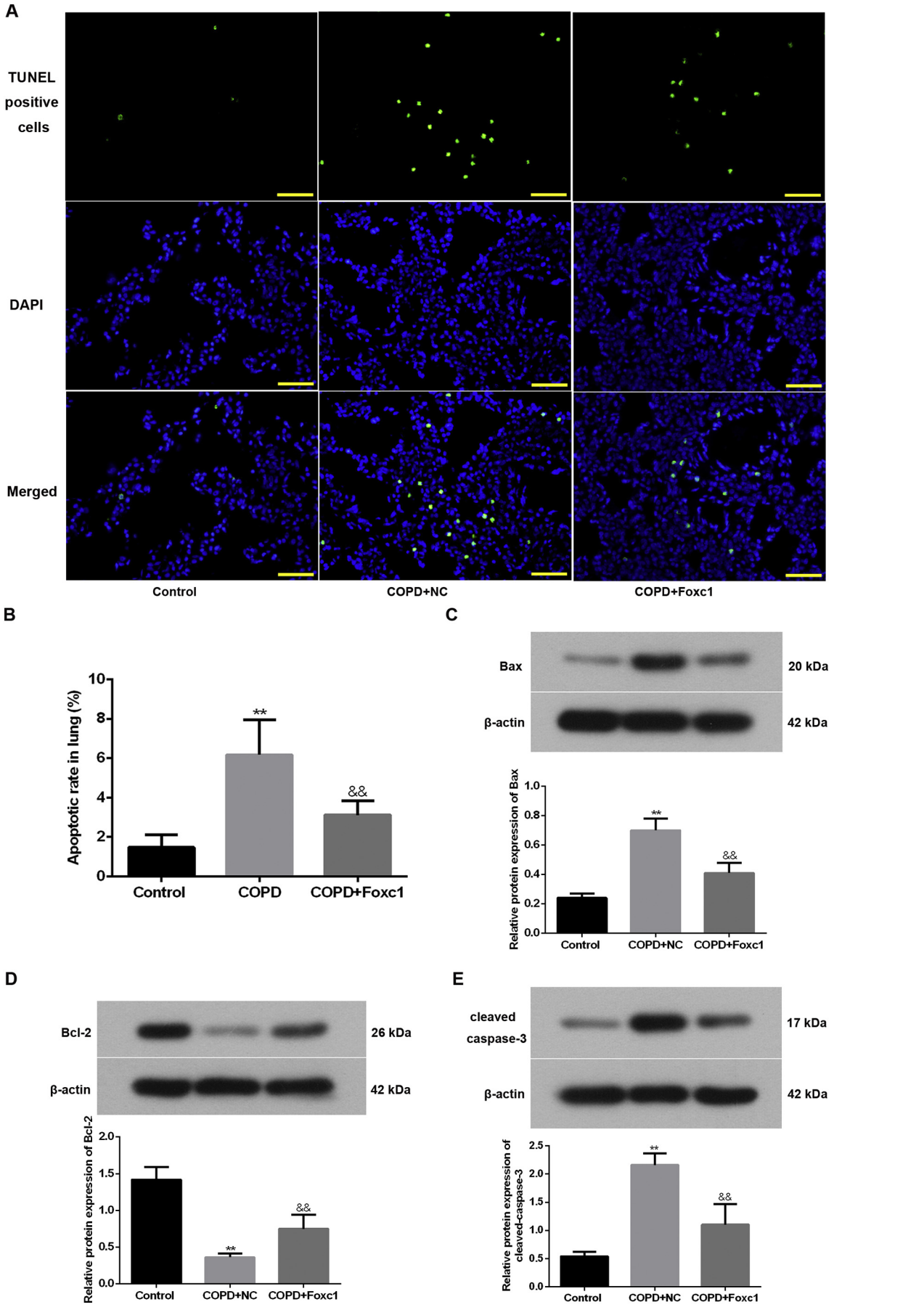

(caption on next page)

Fig. 7. Overexpression of Foxc1 suppressed apoptosis induced by cigarette smoke in lung
Wistar rats with adenovirus carring Foxc1 or negative control were exposed to cigarette smoke or room air for 16 weeks, and the lung tissues were obtained. (A) The apoptosis in the lung in rats exposed to cigarette smoke was assessed by TUNEL and examined under a fluorescence microscope (400× magnification, scale bar: 50 μm). TUNEL positive cells were green staining and DAPI-identified nuclei were blue staining. (B) Percentage of TUNEL positive cells were counted and analyzed. Western blot analysis was used to detect the protein levels of (C) Bax, (D) Bcl-2, and (E) cleaved-caspase-3 in the lung of rats, with β-actin as the internal control. The values are expressed as means ± STDEV (N = 6/group) $^{**}P < 0.01$ vs Control; $^{\&\&}P < 0.01$ vs COPD + NC. (For interpretation of the references to colour in this figure legend, the reader is referred to the web version of this article.)

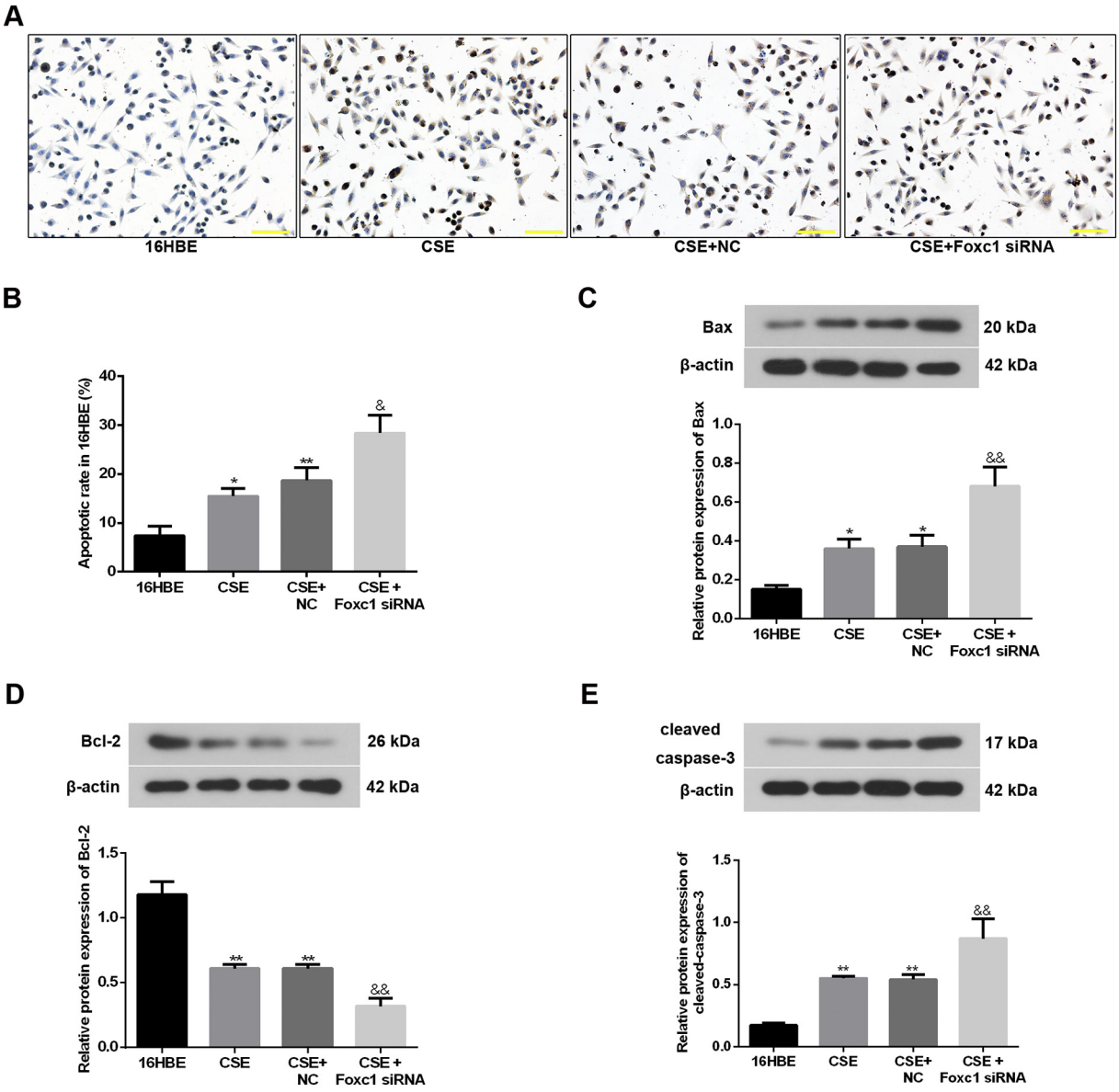

Fig. 8. Knockdown of Foxc1 aggravated apoptosis induced by CSE treatment in 16HBE cells
16HBE cells were transfected with Foxc1 siRNA or negative control sequence. Subsequently, 16HBE cells were incubated in the presence and absence of CSE (10%) for 24 h. (A) The apoptosis in 16HBE cells with CSE treatment was assessed by TUNEL and examined under a microscope (200× magnification, scale bar: 100 μm). TUNEL positive cells were brown-black nuclear stain. (B) Percentage of TUNEL positive cells were counted and analyzed. Western blot analysis was used to detect the protein levels of (C) Bax, (D) Bcl-2, and (E) cleaved-caspase-3 in the 16HBE cells, with β-actin as the internal control. The values are expressed as means ± STDEV (N = 3/group) $^{*}P < 0.05$ vs 16HBE, $^{**}P < 0.01$ vs 16HBE; $^{\&}P < 0.05$ vs CSE + NC, $^{\&\&}P < 0.01$ vs CSE + NC. (For interpretation of the references to colour in this figure legend, the reader is referred to the web version of this article.)

Furthermore, numerous studies demonstrated that Foxc1 resisted apoptosis in human trabecular meshwork cells [17], early Xenopus development [37], and the morphogenesis of the cardiac outflow tract [38]. In accordance with these researches, here we showed cigarette smoke resulted in obvious apoptosis in the lung in COPD rats. Additionally, overexpression of Foxc1 significantly reduced the apoptosis, indicating the beneficial role of Foxc1 in cigarette smoke-induced lung injury. Therefore, we demonstrated that overexpression of Foxc1 alleviated the lung injury in COPD rats induced by cigarette smoke. Furthermore, our results indicated that knockdown of Foxc1 promoted inflammation and oxidative stress, and induced apoptosis in 16HBE cells under CSE treatment, which further verified the protective effect of Foxc1 in COPD. Nevertheless, there are a few notable limitations in the present study. For example, the mechanism of Foxc1 in oxidative

stress and apoptosis in COPD has not been well elucidated, which needs further investigation.

5. Conclusion

Our results delineate a strong association between Foxc1 and the progression of COPD. Foxc1 is upregulated in the lung in COPD rats compared to controls, and overexpression of Foxc1 ameliorated cigarette smoke-induced lung injury, including the mitigation of oxidative stress, inflammation, and apoptosis. Furthermore, downregulation of Foxc1 has the opposite effect in 16HBE cells under CSE treatment. These data suggest that Foxc1 has the potential to serve as a therapeutic target of COPD.

Supplementary data to this article can be found online at https://doi.org/10.1016/j.lfs.2018.11.023.

Acknowledgements

This study was supported by grants from the Science and Technology Special Project for Shenyang Social Development (No. F16-156-9-00), China and the Research Project of Department of Science and Technology, Department of Education of Liaoning Province (No. L2014419), China.

References

[1] M. Maddocks, N. Lovell, S. Booth, W.D. Man, I.J. Higginson, Palliative care and management of troublesome symptoms for people with chronic obstructive pulmonary disease, Lancet 390 (2017) 988–1002.
[2] Global Burden of Disease Study, Global, regional, and national age-sex specific mortality for 264 causes of death, 1980–2016: a systematic analysis for the Global Burden of Disease Study 2016, Lancet 390 (2017) 1151–1210.
[3] Global Burden of Disease Study, Global, regional, and national incidence, prevalence, and years lived with disability for 328 diseases and injuries for 195 countries, 1990–2016: a systematic analysis for the Global Burden of Disease Study 2016, Lancet 390 (2017) 1211–1259.
[4] C.F. Vogelmeier, G.J. Criner, F.J. Martinez, A. Anzueto, P.J. Barnes, J. Bourbeau, et al., Global strategy for the diagnosis, management, and prevention of chronic obstructive lung disease 2017 report. GOLD executive summary, Am. J. Respir. Crit. Care Med. 195 (2017) 557–582.
[5] B. Zhu, Y. Wang, J. Ming, W. Chen, L. Zhang, Disease burden of COPD in China: a systematic review, Int. J. Chron. Obstruct. Pulmon. Dis. 13 (2018) 1353–1364.
[6] R.M. Tuder, I. Petrache, Pathogenesis of chronic obstructive pulmonary disease, J. Clin. Invest. 122 (2012) 2749–2755.
[7] S. Roversi, L.M. Fabbri, D.D. Sin, N.M. Hawkins, A. Agusti, Chronic obstructive pulmonary disease and cardiac diseases. An urgent need for integrated care, Am. J. Respir. Crit. Care Med. 194 (2016) 1319–1336.
[8] R. Kohansal, P. Martinez-Camblor, A. Agusti, A.S. Buist, D.M. Mannino, J.B. Soriano, The natural history of chronic airflow obstruction revisited: an analysis of the Framingham offspring cohort, Am. J. Respir. Crit. Care Med. 180 (2009) 3–10.
[9] Y.P. Wu, C. Cao, Y.F. Wu, M. Li, T.W. Lai, C. Zhu, et al., Activating transcription factor 3 represses cigarette smoke-induced IL6 and IL8 expression via suppressing NF-kappaB activation, Toxicol. Lett. 270 (2017) 17–24.
[10] J. Wang, W. Li, Y. Zhao, Fu Kang, X. Zheng, et al., Members of FOX family could be drug targets of cancers, Pharmacol. Ther. 181 (2018) 183–196.
[11] F.B. Berry, R.A. Saleem, M.A. Walter, FOXC1 transcriptional regulation is mediated by N- and C-terminal activation domains and contains a phosphorylated transcriptional inhibitory domain, J. Biol. Chem. 277 (2002) 10292–10297.
[12] J. Liu, Z. Zhang, X. Li, J. Chen, G. Wang, Z. Tian, et al., Forkhead box C1 promotes colorectal cancer metastasis through transactivating ITGA7 and FGFR4 expression, Oncogene 37 (41) (2018) 5477–5491.
[13] Z. Yang, S. Jiang, Y. Cheng, T. Li, W. Hu, Z. Ma, et al., FOXC1 in cancer development and therapy: deciphering its emerging and divergent roles, Ther. Adv. Med. Oncol. 9 (2017) 797–816.
[14] M. Yoshida, K. Hata, R. Takashima, K. Ono, E. Nakamura, Y. Takahata, et al., The transcription factor Foxc1 is necessary for Ihh-Gli2-regulated endochondral ossification, Nat. Commun. 6 (2015) 6653.
[15] P. Xu, B. Balczerski, A. Ciozda, K. Louie, V. Oralova, A. Huysseune, et al., Fox proteins are modular competency factors for facial cartilage and tooth specification, Development 145 (2018).
[16] F.B. Berry, J.M. Skarie, F. Mirzayans, Y. Fortin, T.J. Hudson, V. Raymond, et al., FOXC1 is required for cell viability and resistance to oxidative stress in the eye through the transcriptional regulation of FOXO1A, Hum. Mol. Genet. 17 (2008) 490–505.
[17] Y.A. Ito, I.S. Goping, F. Berry, M.A. Walter, Dysfunction of the stress-responsive FOXC1 transcription factor contributes to the earlier-onset glaucoma observed in Axenfeld-Rieger syndrome patients, Cell Death Dis. 5 (2014) e1069.
[18] A. Kotanidou, H. Loutrari, E. Papadomichelakis, C. Glynos, C. Magkou, A. Armaganidis, et al., Inhaled activated protein C attenuates lung injury induced by aerosolized endotoxin in mice, Vasc. Pharmacol. 45 (2006) 134–140.
[19] I. Heijink, A. van Oosterhout, N. Kliphuis, M. Jonker, R. Hoffmann, E. Telenga, et al., Oxidant-induced corticosteroid unresponsiveness in human bronchial epithelial cells, Thorax 69 (2014) 5–13.
[20] D. Morse, I.O. Rosas, Tobacco smoke-induced lung fibrosis and emphysema, Annu. Rev. Physiol. 76 (2014) 493–513.
[21] M.B. Miller, Y.W. Tang, Basic concepts of microarrays and potential applications in clinical microbiology, Clin. Microbiol. Rev. 22 (2009) 611–633.
[22] K. Mirnics, J. Pevsner, Progress in the use of microarray technology to study the neurobiology of disease, Nat. Neurosci. 7 (2004) 434–439.
[23] P.S. Ray, J. Wang, Y. Qu, M.S. Sim, J. Shamonki, S.P. Bagaria, et al., FOXC1 is a potential prognostic biomarker with functional significance in basal-like breast cancer, Cancer Res. 70 (2010) 3870–3876.
[24] L. Xia, W. Huang, D. Tian, H. Zhu, X. Qi, Z. Chen, et al., Overexpression of forkhead box C1 promotes tumor metastasis and indicates poor prognosis in hepatocellular carcinoma, Hepatology 57 (2013) 610–624.
[25] L. Wang, L. Chai, Q. Ji, R. Cheng, J. Wang, S. Han, Forkhead box protein C1 promotes cell proliferation and invasion in human cervical cancer, Mol. Med. Rep. 17 (2018) 4392–4398.
[26] Q. Lu, E. Gottlieb, S. Rounds, Effects of cigarette smoke on pulmonary endothelial cells, Am. J. Physiol. Lung Cell. Mol. Physiol. 314 (2018) L743–L756.
[27] S. Boukhenouna, M.A. Wilson, K. Bahmed, B. Kosmider, Reactive oxygen species in chronic obstructive pulmonary disease, Oxidative Med. Cell. Longev. 2018 (2018) 5730395.
[28] Z. Meiqian, Z. Leying, C. Chang, Astragaloside IV inhibits cigarette smoke-induced pulmonary inflammation in mice, Inflammation, 2018.
[29] P. Paliogiannis, A.G. Fois, S. Sotgia, A.A. Mangoni, E. Zinellu, P. Pirina, et al., Circulating malondialdehyde concentrations in patients with stable chronic obstructive pulmonary disease: a systematic review and meta-analysis, Biomark. Med 12 (2018) 771–781.
[30] L. Ni, C. Dong, Roles of myeloid and lymphoid cells in the pathogenesis of chronic obstructive pulmonary disease, Front. Immunol. 9 (2018) 1431.
[31] J. Sonett, M. Goldklang, P. Sklepkiewicz, A. Gerber, J. Trischler, T. Zelonina, et al., A critical role for ABC transporters in persistent lung inflammation in the development of emphysema after smoke exposure, FASEB J. (2018) fj201701381, , https://doi.org/10.1096/fj.201701381 [Epub ahead of print].
[32] I.K. Demedts, T. Demoor, K.R. Bracke, G.F. Joos, G.G. Brusselle, Role of apoptosis in the pathogenesis of COPD and pulmonary emphysema, Respir. Res. 7 (2006) 53.
[33] R.J. Giordano, J. Lahdenranta, L. Zhen, U. Chukwueke, I. Petrache, R.R. Langley, et al., Targeted induction of lung endothelial cell apoptosis causes emphysema-like changes in the mouse, J. Biol. Chem. 283 (2008) 29447–29460.
[34] T. Goldkorn, S. Filosto, S. Chung, Lung injury and lung cancer caused by cigarette smoke-induced oxidative stress: molecular mechanisms and therapeutic opportunities involving the ceramide-generating machinery and epidermal growth factor receptor, Antioxid. Redox Signal. 21 (2014) 2149–2174.
[35] A. Kaplan, G. Akalin Ciftci, H.M. Kutlu, The apoptotic and genomic studies on A549 cell line induced by silver nitrate, Tumor Biol. 39 (2017) (1010428317695033).
[36] W.W. Wang, B. Chen, C.B. Lei, G.X. Liu, Y.G. Wang, C. Yi, et al., miR-582-5p inhibits invasion and migration of salivary adenoid cystic carcinoma cells by targeting FOXC1, Jpn. J. Clin. Oncol. 47 (2017) 690–698.
[37] J.Y. Cha, B. Birsoy, M. Kofron, E. Mahoney, S. Lang, C. Wylie, et al., The role of FoxC1 in early *Xenopus* development, Dev. Dyn. 236 (2007) 2731–2741.
[38] S. Seo, T. Kume, Forkhead transcription factors, Foxc1 and Foxc2, are required for the morphogenesis of the cardiac outflow tract, Dev. Biol. 296 (2006) 421–436.